DOI: 10.1002/ejic.200801114

Hydrotalcite-Like Nanocrystals from Water-in-Oil Microemulsions

Francesca Bellezza,[a] Antonio Cipiciani,*[a] Umberto Costantino,[a] Morena Nocchetti,[a] and Tamara Posati[a]

Keywords: Microreactors / Micelles / Nanostructures / Layered compounds / Hydrotalcite-like compounds

A water-in-oil microemulsion made up of a cetyltrimethylammonium bromide/*n*-butanol/isooctane/M^{II} and Al^{III} nitrate aqueous solution (M^{II} = Mg or Ni or Zn) has been mixed with a microemulsion of the same composition but containing an ammonia solution instead of a metal nitrate solution. Collisions between the reverse micelles containing an M^{II} and Al^{III} solution and those containing an NH_3 solution form short-lived dimers that act as reaction vessels and control the nucleation and growth of MgAl, NiAl or ZnAl hydrotalcite-like compounds (HTlcs). The double water-in-oil microemulsion technique yields colloidal dispersions of nanoparticles whose size and shape were examined by transmission electron microscopy (TEM) and atomic force microscopy (AFM). The colloidal particles were between 50 and 100 nm depending on the composition of the microemulsions (water-to-surfactant and oil-to-water molar ratios). The separation of the nanoparticles from the reaction medium produces a gel made up of surfactant-free particles. HTlc nanocrystals were recovered from the gel (reaction medium), washed, and dried. They were then studied by chemical and thermogravimetric analyses, X-ray powder diffraction, N_2-adsorption and BET surface analysis and scanning electron microscopy (SEM). The $Al^{III}/(M^{II} + Al^{III})$ molar ratio of the recovered HTlc nanocrystals was between 0.24 and 0.29, and the basal spacing was about 8 Å, a value in agreement with the presence of charge compensating bromide anions in the interlayer region. The proposed technique allows for HTlc nanocrystals to be obtained with a relatively high surface area with values ranging between 50 and 110 m^2/g. The SEM analyses show that the nanoparticles are aggregated to give rise to complex spherical or rod-shaped microstructures.

Introduction

Nanoscience and nanotechnology have developed rapidly, and there are now synthetic procedures for obtaining functional materials at the nanometre scale that are of interest in physical, chemical and biomedical applications.[1] The synthesis of hydrotalcite-like compounds (HTlcs) having a crystallite size in the nanometre range with a very limited size distribution is currently being studied. HTlcs, derived from the mineral hydrotalcite, $Mg_6Al_2(OH)_{16}CO_3{\cdot}4H_2O$,[2] consist of stacked layers having a brucitic structure that are positively charged because of the partial substitution of divalent cations with trivalent cations. The anions are set in the interlayer galleries in order to maintain overall charge neutrality and to link the adjacent layers through ionic bonds.

The hydrotalcite-like compounds are also known as "anionic clays" or "layered double hydroxides." Their empirical formula is $[M^{II}_{1-x}M^{III}_x(OH)_2]^{x+}[A^{n-}_{x/n}]^{x-}{\cdot}mH_2O$, where M^{II} is a divalent cation such as Mg, Zn, Ni, Co or Cu, M^{III} is a trivalent cation such as Al, Cr, Fe or Ga, A^{n-} is an anion of charge n and m is the molar amount of co-intercalated water. The x values generally range between 0.2 and 0.4 and determine the charge density of the positive layer and the anion exchange capacity.[3] The charge-balancing anions can be exchanged by other inorganic, organic or metallo-organic anions to obtain functional materials that are of interest in the fields of photophysics and photochemistry,[4] catalysis,[5] drug storage and release, cosmetics,[6] additives and polymer fillers.[7]

While much information is available in the literature regarding the physicochemical properties and above-mentioned applications of HTlcs, relatively few reports are concerned with methods for controlling the particle size and particle size distribution at the nanometre scale. The few reported attempts are based on controlling nucleation and crystal growth using conventional synthetic procedures[8] by varying parameters such as metal ion concentration, addition rate, temperature, aging time and the nature of the precipitating reagent.

Very few papers report HTlc synthesis based on water-in-oil microemulsions,[9] even though this synthetic procedure has been widely used to prepare colloidal inorganic nanocrystals.[10] The microemulsions can be considered as nanosized reaction chambers that are well-suited for controlling the nucleation and growth of inorganic precipi-

[a] Centro di Eccellenza Materiali Innovativi Nanostrutturati (CEMIN), Dipartimento di Chimica, Università di Perugia, Via Elce di Sotto, 8, 06123 Perugia, Italy
Fax: +39-075-5855560
E-mail: cipan@unipg.it

Supporting information for this article is available on the WWW under http://www.eurjic.org or from the author.

tates.[11] Water-in-oil microemulsions are transparent, isotropic liquid media that contain very small water droplets dispersed in a continuous oil phase; they are stabilized by surfactant and cosurfactant molecules at the water/oil interface. The water droplets, surrounded by surfactant molecules, offer a unique microenvironment for the formation of nanoparticles. Not only do they act as microreactors for processing reactions, but they also control the aggregation of particles since the surfactant molecules can be adsorbed onto the particle surface when the particle size approaches that of the water pool.

The above-mentioned studies describe the synthesis of MgAl HTlc nanocrystals in a water-in-oil microemulsion of sodium lauryl sulfate, an anionic surfactant, water and isooctane. The system yielded nanometre-sized HTlc particles, with a 40–50 nm diameter and 10 nm thickness, containing the anionic surfactant as counterion.[9] Moreover, the addition of triblock copolymers during the crystallization step allowed different growth orientations of the HTlc structure to be obtained.[9] Furthermore, Liu and coworkers used a microemulsion method to synthesize NiMgAl HTlc particles as a precursor to nickel-supporting catalysts of alkanol-reforming reactions.[9d]

This paper reports the preparation and characterization of MgAl, NiAl and ZnAl hydrotalcite-like compounds by using the double-microemulsion technique with a cationic surfactant. With this technique, two microemulsions are mixed, each containing one of the reactants that form the precipitate, and the intermicellar exchange of solutes is essential to the formation of the product.[12] The droplets, subject to Brownian motion, continuously collide to lead to the formation of short-lived dimers, and the aqueous contents of the reverse micelles mix. This dynamic process ensures a homogeneous repartitioning of the reactants among the water pools of the droplets and thus the formation of monodispersed particles (see Scheme in Figure 1).

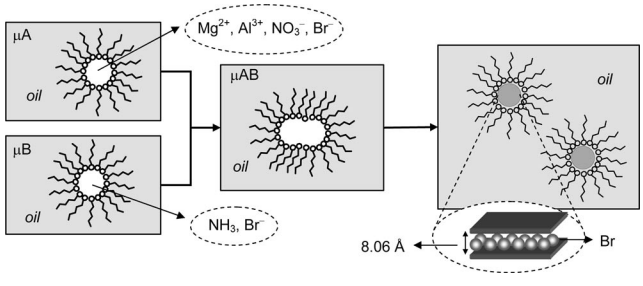

Figure 1. Steps involved in the double-microemulsion technique used to synthesize the HTlc nanoparticles.

A typical quaternary water-in-oil microemulsion of cetyltrimethylammonium bromide (CTABr)/*n*-butanol/isooctane/water was used in the present work. The use of a cationic surfactant has a double benefit. First, it avoids the complication of eliminating the surfactant from the obtained particles that have an anion exchange property. Second, it allows the HTlc to be obtained in bromide form. This is considered a good precursor for intercalating other anionic species – even of large dimensions – by ion exchange. The particle size of the obtained HTlc dispersion was investigated by transmission electron microscopy (TEM) and atomic force microscopy (AFM). The nanocrystals recovered from the reaction media were dried and then studied by chemical and thermogravimetric analyses, scanning electron microscopy (SEM), X-ray powder diffraction (XRPD), BET surface analysis and porosity.

Results and Discussion

Synthesis of MgAl HTlc Nanoparticles by the Double-Microemulsion Technique

First, the optimization of the synthetic parameters for obtaining MgAl HTlc nanoparticles in reverse micelles with the double-microemulsion technique will be described. As shown in Figure 1, the precipitation reaction takes place in the core of the reverse micelles, and when the size of the precipitate approaches the size of the water pool, the interactions between the particle surface and the hydrophilic head groups of the surfactant may stop the nanoparticle growth.

It is known that the size of microemulsion droplets depends on the composition of the solution.[13] To a first approximation, the amount of water influences the droplet size because it depends on the water-to-surfactant molar ratio, R_w.

$$R_w = n\,(H_2O)/n\,(\text{Surfactant})$$

The average diameter of the microemulsion droplets increases as the water content increases because of an increase in the total volume of water and a concomitant decrease in the total surface area of the aggregate. The ability of the surfactant–alkane mixtures to solubilize water is limited and varies depending on the surfactant structure, oil phase and temperature. The R_w values alone are not enough to characterize the microemulsion system. The oil-to-water molar ratio, R_o, is another important parameter which affects micelle formation.

$$R_o = n\,(\text{Oil})/n\,(H_2O)$$

The presence of cosurfactant, as in the quaternary microemulsion system, may have a significant effect on the interfacial property of the droplets.

Several experiments were carried out in which the relative amounts of oil, water, surfactant and cosurfactant were varied in order to obtain clear, stable microemulsions. The composition of microemulsions containing either Mg^{II} and Al^{III} nitrates or NH_3 as the precipitating agent (A and B, respectively) are listed in Table 1 [note that the surfactant/cosurfactant (w/w) ratio was kept constant and equal to 1]. In all of the experiments the mixtures obtained by mixing microemulsions A and B remained transparent for ca 15 min, after which they became cloudy. They were then aged at 75 °C for 15 h (or 8 h) or at 25 °C for 15 h. The precipitation of HTlc particles was expected to take place in the nanosized aqueous domains; it probably occurred soon after the two highly supersaturated microemulsions

Table 1. Composition of the microemulsions (μE), temperature and reaction time used for the synthesis of MgAl HTlc nanoparticles.

Sample	μE[a]	[S][b] (wt.-%)	[O][b] (wt.-%)	[W][b] (wt.-%)	[C][b] (wt.-%)	R_w	R_o	t [h]	T [°C]
1	A	23	46	8	23	7	0.9	15	75
	B	23	46	8	23	7	0.9		
2	A	22	44	12	22	11	0.6	15	75
	B	22	44	12	22	11	0.6		
3	A	20	39	21	20	21	0.3	15	75
	B	20	39	21	20	21	0.3		
4	A	18	37	27	18	30	0.2	15	75
	B	18	37	27	18	30	0.2		
5	A	20	39	21	20	21	0.3	15	25
	B	20	39	21	20	21	0.3		
6	A	20	39	21	20	21	0.3	8	75
	B	20	39	21	20	21	0.3		

[a] A: $[Mg(NO_3)_2]$ = 0.4 M, $[Al(NO_3)_3]$ = 0.125 M; B: $[NH_3]$ = 5.0 M. [b] S = surfactant (CTABr), O = oil (isooctane), W = water, C = cosurfactant (*n*-butanol).

were mixed. The results of these experiments show that it is possible to obtain HTlc particles over a large range of R_o and R_w values. These particles can be collected by centrifugation.

Figure 2 shows the XRPD patterns of the centrifuged and dried samples listed in Table 1. The sample patterns exhibit the typical reflections of the hydrotalcite structure. The peaks were indexed by comparing them with the patterns of microcrystalline MgAl HTlc in chloride form, which has already been indexed based on its structural parameters.[14] All of the samples were characterized by an identical interlayer distance (8.06 Å), which is compatible with the presence of bromide charge-compensating anions in the interlayer region.[3a]

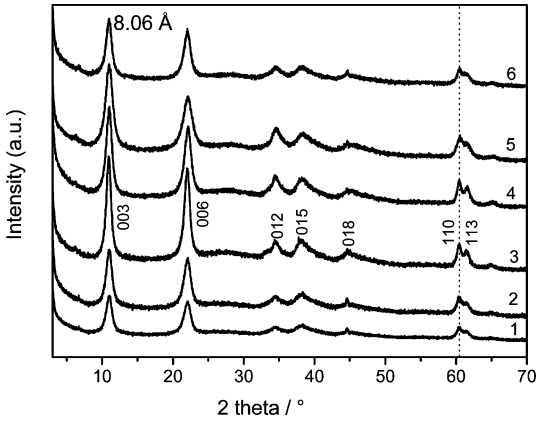

Figure 2. XRPD patterns of the MgAl HTlc samples 1–6 reported in Table 1.

The broadening and resolution of the diffraction peaks give an indication of the degree of crystallinity of the samples, which is affected by the conditions under which they were synthesized. In particular, as the R_w values, reaction times and temperatures increase (see samples 3 and 4), the crystallinity increases. The (110) and (113) diffraction lines become broader and overlap for samples 1 and 2 (low R_w values) and samples 5 and 6 (short reaction times and low temperatures).

Moreover, the d value of the (110) X-ray diffraction maximum allows the cell parameter a to be determined [$a = 2 \times d_{(110)} = 3.064(6)$ Å]. The value is in good agreement with those reported in previous works.[14] For all of the synthesized samples, the $d_{(110)}$ value, which depends on the Mg/Al molar ratio, is almost the same. This result shows that the reaction conditions did not significantly affect the composition of the solids.

An Al/(Al + Mg) molar fraction of 0.29 was determined by ICP analysis for sample 3. This value was a little higher than that expected for the solution of microemulsion A, but was close to that of the hydrotalcite mineral. It should be noted that bromide anions present in the water pool of the reverse micelles as counterions of the surfactant (CTABr), together with bivalent and trivalent metal cations and nitrate anions (see Figure 1), are preferentially intercalated during the precipitation of the hydrotalcites. The presence of easily exchangeable Br^- counterions allows for a one-pot functionalization of the lamellar solids with other inorganic or organic anions. This is in contrast to what occurs when HTlcs in the carbonate form are used.[6a]

The sample compositions were assigned with a combination of thermogravimetric analysis, used to study the thermal behaviour, and ion chromatography. Figure 3 shows the coupled TG/DTA curves for sample 3. The curves can be divided into two well-differentiated regions: the first region, ranging from 80 to 220 °C, shows a broad endothermic peak related to the dehydration of the sample; the second, ranging from 220 to 800 °C, corresponds to the weight loss due to dehydroxylation and the loss of bromide and carbonate counteranions. Given the Mg/Al and Al/Br molar ratios and the fact that MgO and $MgAl_2O_4$ are formed at 1000 °C, it was possible to assign the following composition to sample 3: $[Mg_{0.71}Al_{0.29}(OH)_2]Br_{0.19}(CO_3)_{0.05}\cdot 0.69H_2O$.

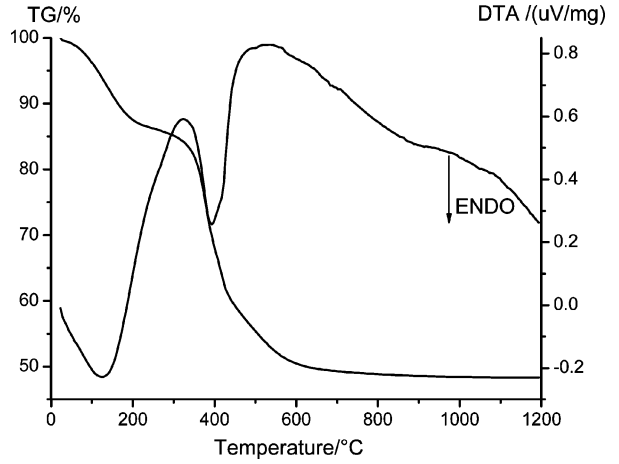

Figure 3. TG/DTA curves of sample 3 from Table 1. (Operative conditions: heating rate: 10 °C/min, air flow).

Figure 3 and the TG/DTA curves obtained for the other samples (see Figure S1) do not show any weight loss associated with exothermic peaks, which is typical of the combustion of adsorbed and/or intercalated organic moieties. This finding indicates that the HTlc nanocrystals prepared by using a cationic surfactant do not contain adsorbed and/or intercalated residual surfactant species. The absence of surfactant species in the synthesized materials was also confirmed by elemental analysis. The carbon content for sample 3 was only 0.64% (w/w); this value was very close to that calculated on the basis of the previously assigned formula [0.67% (w/w)]. Therefore, by using a cationic surfactant instead of an anionic one, as reported in previous works,[9] surfactant-free HTlc can be obtained that can be used directly as a host for anionic species.

Table 2 reports the BET surface area of the MgAl HTlc particles obtained by the double-microemulsion technique. The adsorption and desorption isotherms (data not shown) exhibit a large hysteresis loop; the shape is the same type (IV) as that observed for most mesoporous materials. The mean value and width of the pore size distribution extracted from the BJH[15] method for desorption branch and mesopore volume are also reported in Table 2. The samples have a relatively large surface area, ranging from about 50 to 110 m^2/g. All of the samples exhibit a mesoporosity that can be ascribed to the particle aggregation that forms a house of cards. It should be noted that the BET surface area values are higher than those of microcrystalline MgAl HTlcs obtained with conventional coprecipitation (61–88 m^2/g)[16] or urea methods (24 m^2/g).[14]

To evaluate the size distribution of the colloidal dispersion of MgAl HTlc particles, light scattering measurements and TEM images were collected. The particle size distribution for sample 3 (Table 1), determined by a laser light scattering method, was very narrow (80–120 nm) (data not shown).

Figure 4 shows the TEM image of sample 3 obtained from the experiment described in Table 1. The particles were of nanometre size with a uniform width ranging from 70 to 90 nm. They were smooth, well-formed, hexagonal crystals. Figure 4 (B) shows the TEM image of one platelet of sample 3, and the inset shows the corresponding selected-area electron diffraction (SAED) pattern. Hexagonally arranged bright spots are present and confirm the highly single-crystalline nature of the sample. An *a* value of about 3 Å for the hexagonal lattice is compatible with the *in plane* structural parameter of sample 3, determined from the X-ray powder diffraction patterns. The TEM images of other samples obtained in microemulsions characterized by different R_w and R_o values (data not shown) clearly show a platelet structure that is characteristic of HTlcs; the sizes ranged from 40 to 200 nm.

The results (see Tables 1 and 2) show that with a high isooctane/water molar ratio there is a large size distribution of HTlc particles, while a lower isooctane/water ratio and higher water/CTABr ratio produce a narrow size distribution of particles. Note that, under the same R_w and R_o molar ratios, a decrease in both temperature and reaction time produces a wider range of nanoparticle sizes (samples 5 and 6).

Synthesis of NiAl and ZnAl HTlc Nanoparticles with the Double-Microemulsion Technique

Based on the above-described experiments, the parameters used to synthesize MgAl HTlc particles (sample 3 of Table 1) gave the best results in term of XRPD patterns, BET surface area and size distribution of the HTlc particles. The synthesis conditions for sample 3 were then applied to hydrotalcites containing different divalent metal cations such as Ni^{II} and Zn^{II}, while the trivalent cation (Al^{III}) was fixed. Preliminary attempts to synthesize NiAl HTlc nanoparticles under the experimental conditions used for sample 3 gave blue mother water. This result indicated

Table 2. Characterization of MgAl HTlcs nanoparticles.

Sample	BET surface area [m^2/g]	Nanoparticle diameter range [nm][a]	Mesopore volume [cm^3/g]	Pore diameter distribution [nm]
1	101	40–200	0.14	4.5 ± 0.5
2	70	80–200	0.18	5.0 ± 1.5
3	97	70–90	0.19	8.0 ± 3.0
4	110	70–150	0.29	8.8 ± 2.0
5	50	80–200	0.09	3.5 ± 2.0
6	57	80–150	0.08	3.0 ± 1.5

[a] Determined by TEM.

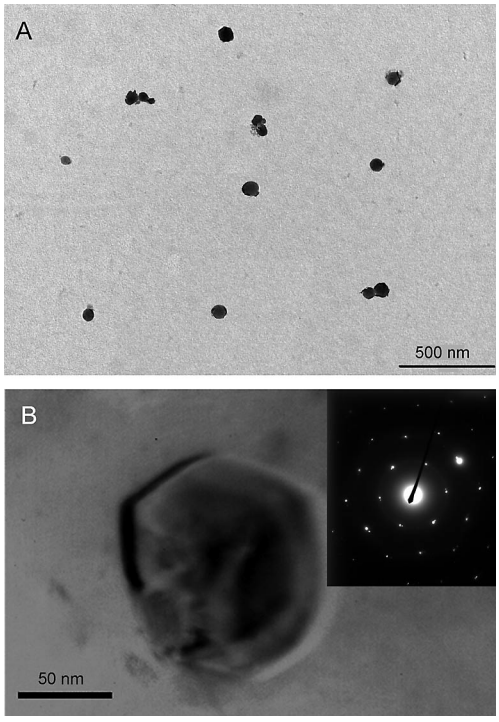

Figure 4. TEM micrograph of sample 3 (A) and selected-area electron diffraction pattern (SAED) of one platelet of sample 3 (B).

the formation of nickel ammoniacal complexes. To avoid this effect, the molar concentration of the ammonia in microemulsion B was decreased stepwise from 5.0 M to 1.25 M until a green gel and colourless mother water were obtained. The same molar concentration of ammonia was used to precipitate the ZnAl HTlc particles.

The X-ray diffraction patterns of the NiAl and ZnAl HTlc nanocrystals are shown in Figure 5. The samples are characterized by a typical hydrotalcite pattern in which the (110) reflection is also present, even though their degree of crystallinity is lower than that of the MgAl HTlc. The sample composition is reported (Table 3) in terms of the empirical formula determined by elemental analysis, ion chromatography and thermogravimetrical analysis. The BET surface area is also given. In contrast to the MgAl and NiAl HTlc particles, only bromide anions were present in the interlayer region in the ZnAl HTlc particles.

The TG/DTA curves of the NiAl and ZnAl HTlc nanocrystals are reported up to 1200 °C (Figure 6). Three stages of endothermic weight loss are evident in both samples. For the NiAl analogue (Figure 6, A), the first step, ranging from 80 °C to 250 °C, is due to the dehydration of the sample and to the decomposition of co-intercalated carbonate anions (see Table 3). For the ZnAl analogue (Figure 6, B),

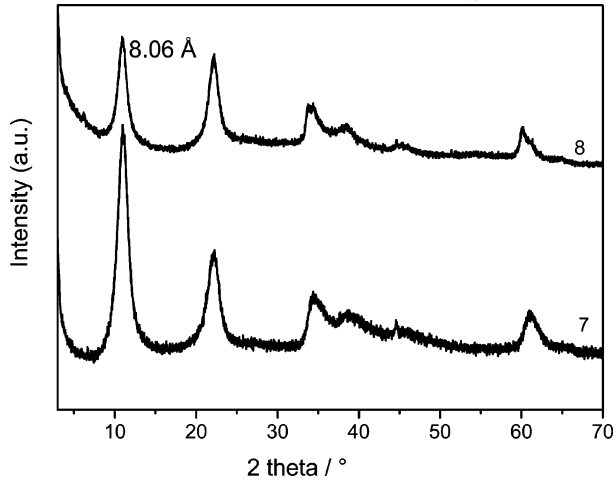

Figure 5. XRPD patterns of NiAl HTlc (sample 7) and ZnAl HTlc (sample 8) reported in Table 3.

the first step, ranging from 80 °C to 150 °C, can be assigned to dehydration. The second region, up to 350 °C, corre-

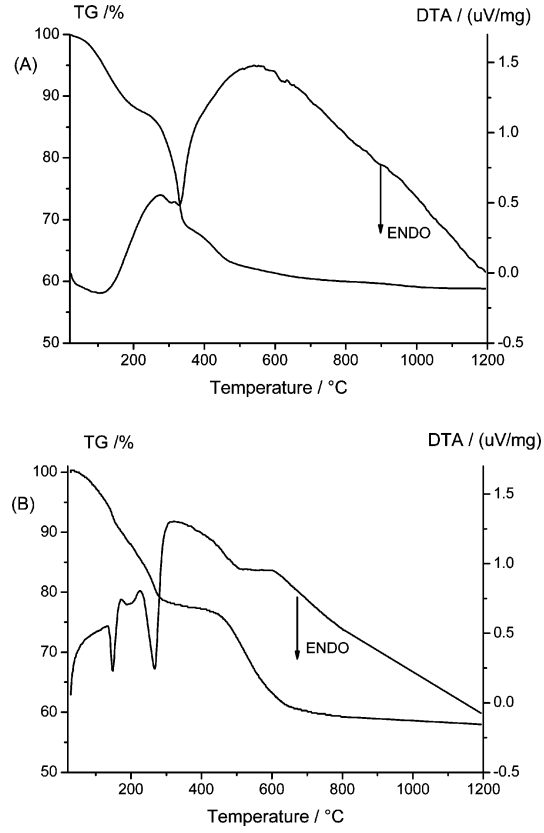

Figure 6. TG/DTA curves of sample 7 (A) and sample 8 (B) from Table 3. (Operative conditions: heating rate: 10 °C/min, air flow).

Table 3. Characterization of NiAl and ZnAl HTlc nanoparticles.

Sample	Composition	BET surface area [m^2/g]	Mesopore volume [cm^3/g]	Pore diameter distribution [nm]
7	$[Ni_{0.77}Al_{0.23}(OH)_2]Br_{0.15}(CO_3)_{0.04}{\cdot}0.81H_2O$	52	0.06	4.0 ± 0.5
8	$[Zn_{0.72}Al_{0.28}(OH)_2]Br_{0.28}{\cdot}0.69H_2O$	20	0.08	7.5 ± 3.0

sponds to the weight loss due to the dehydroxylation of the brucite layers. The last step for the two samples is related to the loss of bromide anions. Again, the exothermic peaks related to the combustion of the organic moieties are absent, which indicates the absence of adsorbed surfactant species. The calculated carbon content of samples 7 and 8, determined on the basis of the formulae reported in Table 3, were 0.42 and 0%, in agreement with the experimental values found by elemental analysis (0.48 and 0.1%, respectively). The surface areas were lower than those of most of the MgAl HTlc particles and were very close to those of microcrystalline hydrotalcites obtained by the urea method.[14]

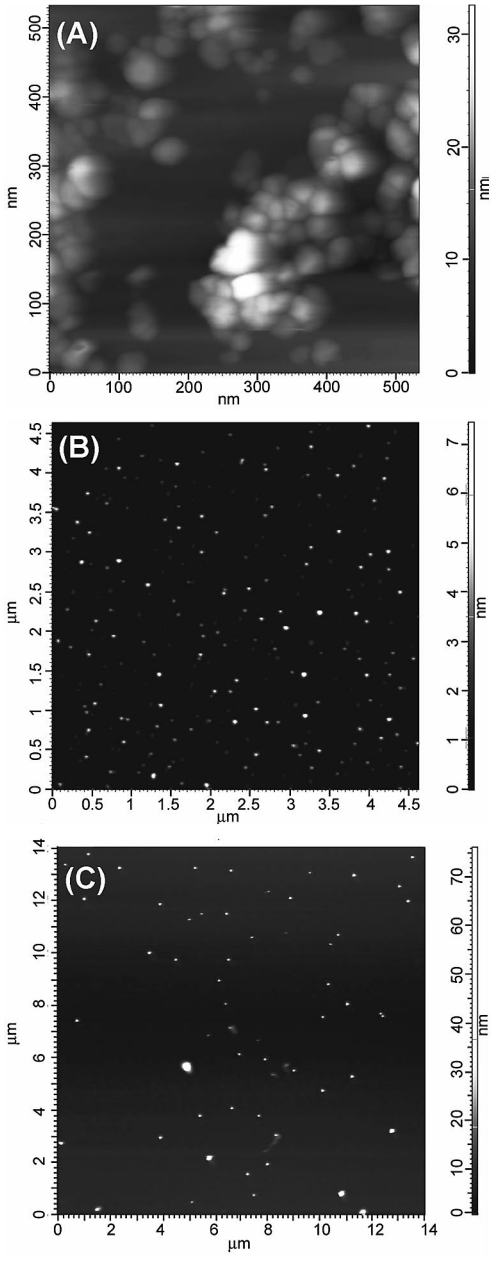

Figure 7. 2D AFM images of sample 3 (A), sample 7 (B) and sample 8 (C).

AFM Imaging of HTlc Nanoparticles

While the TEM micrographs gave clear indications about the nanoscale size of the synthesized HTlcs, it was of interest to investigate the materials by using AFM. AFM in tapping mode has become a powerful tool for obtaining real-space high-resolution images of individual particles; it provides geometric information that is not easily accessible by electron microscopy. AFM studies of HTlc materials have shown that this technique can be used to characterize structurally delicate and beam-sensitive materials.[9]

2D topographic maps of sample 3, representative of MgAl HTlcs, and of samples 7 and 8, representative of NiAl and ZnAl HTlcs respectively, show clearly resolved isolated particles (Figure 7). Even though some aggregates were observed by AFM, they were not taken into account when the size distribution was determined. The images suggest that the particles have different thicknesses and a more homogeneous diameter distribution.

The average diameter and probable thickness of the samples are reported in Table 4; the thickness was compared with the value obtained by applying the Debye–Scherrer equation to the (00*l*) Bragg reflections. The calculated diameter is not reported because of the low (110) reflection intensity. The overlap with the (113) reflection, coupled with the approximations intrinsic in the Debye–Scherrer equation, lead to some uncertainty about the calculated crystal size in the *a* direction. Note that the calculated and measured thickness values of samples 3 and 7 are in good agreement with each other. Furthermore, the diameter of sample 3 determined by AFM was close to that determined by TEM (see Figure 4).

SEM Imaging of HTlc Nanoparticles

The morphology and organization of the nanoparticles, recovered after centrifuging and dispersed in water, acetone or a chloroform/methanol mixture (see experimental section), were investigated by SEM. Figure 8 shows the SEM images of samples 7 and 8 dispersed in water; interesting morphological features are evident.

The MgAl and NiAl HTlc particles (samples 3 and 7) form spherical clusters with a diameter of about 2–3 µm (Figure 8, A). The formation of such microspheres is not easily explained; the small platelets of hydrotalcite in water probably migrate on the surface of water droplets during the evaporation process of the solvent and aggregate to assume the spherical droplet shape. Furthermore, the microsphere surface is smooth, which is probably due to the small platelet size and their ordered packing. Micro- and nanospheres were also found during the HTlc synthesis as reported by other authors such as R. Xu and al.[8h] and C.G. Zhang and al.[17] The ZnAl HTlc particles had another type of organization which formed rod-like structures in which the single nanocrystals were aggregated along a preferential direction (Figure 8, B).

Samples obtained from gels dispersed in acetone or in a chloroform/methanol mixture were characterized by a

Table 4. Characterization of MgAl (sample 3), NiAl (sample 7) and ZnAl (sample 8) HTlc nanoparticles.

Sample	Measured particle size[a] Thickness [nm]	Diameter [nm]	(003) and (006) Bragg reflections 2θ [°]	FWHM [°]	Calculated thickness [nm][b]
3	5 ± 2	60 ± 5	10.95	0.80	9.9
			22.03	0.90	9.0
7	3.5 ± 1	44 ± 10	11.05	1.53	5.2
			22.07	1.72	4.7
8	30 ± 15	150 ± 50	10.99	1.24	6.4
			22.19	1.45	5.6

[a] By AFM. [b] By Debye–Scherrer equation: $D = 0.9 \times \lambda/(\delta \times \cos\theta)$ (λ = incident ray wavelength: 1.54050 Å; δ = FWHM; θ = diffraction angle).

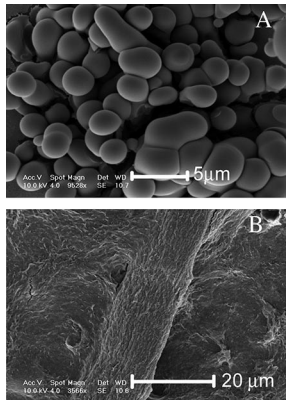

Figure 8. SEM micrographs at different magnitudes of sample 7 (A) and sample 8 (B) obtained by drying the corresponding gels dispersed in water.

background made up of dense aggregates of platelet-like structures which contain rare clusters of microspheres and rod-like structures. The capacity to aggregate decreased in all the samples when the washing solvent was changed from water to organic solvents. This could have been due to differences in the solvent–nanoparticle interaction. Moreover,

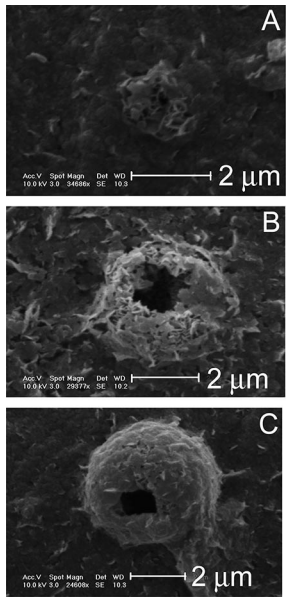

Figure 9. SEM micrographs of sample 8 at different magnitudes obtained by drying the corresponding gel dispersed in acetone.

new globular structures in which the surface was clearly made up of assembled nanocrystals were found in ZnAl HTlc samples. Figure 9 shows a sequence of micrographs that show the formation of the globular aggregates. The formation mechanism of the holes on the globular surfaces is not clear. They may have been formed by a higher rate of solvent evaporation.

Therefore, the properties of the solvent chosen to obtain the dispersion, the nanoparticle size and, very likely, the type of interaction between the nanoplatelets, produce different morphologies of the final ordered aggregates. This is in agreement with observations by other authors.[1b]

Finally, it should be noted that instrumental resolution does not always allow the single nanoplatelets to be identified. Where it was possible, the width determined by SEM was in agreement with that obtained by TEM and AFM.

Conclusions

Nanosized MgAl, NiAl and ZnAl HTlc particles can be prepared in cationic water-in-oil microemulsions of water/CTABr/*n*-butanol/isooctane using $M(NO_3)_2$ (M = Mg, Zn or Ni), $Al(NO_3)_3$ and NH_3 as reagents. The nanoparticles are rapidly formed and are stable over time. The size of the colloidal particles can be controlled by the composition of the microemulsion. A high isooctane/water molar ratio produces a large size distribution of HTlc particles, while lower isooctane/water and higher water/CTABr produce a narrow size distribution of particles. Under the same R_w and R_o molar ratios, a decrease in both temperature and reaction time produces a broader nanoparticle dimension range. The separation of the nanoparticles from the reaction medium produces a stable gel made up of surfactant-free nanoparticles.

The bromide anions present in the water pool of the reverse micelles as counterions of the surfactant (CTABr), together with the bivalent and trivalent metal cations and the nitrate anions, are preferentially intercalated during the precipitation of the HTlc nanoparticles. The presence of easily exchangeable bromide counterions allows for the lamellar solids to be directly functionalized with other inorganic or organic anions.

The results of this study show that it is relatively easy to obtain a wide variety of M^{II}–Al^{III} HTlc nanoparticles; this will allow hydrotalcite materials to be developed in several nanotechnological fields.

Experimental Section

Chemicals: Cetyltrimethylammonium bromide was supplied by Aldrich. All other reagents were C. Erba RP-ACS products.

Synthesis of HTlc Nanoparticles by the Microemulsion Technique: Cetyltrimethylammonium bromide as surfactant, *n*-butanol as cosurfactant and isooctane as the oil phase were used to prepare the microemulsions.

Two microemulsions, designated A and B, with identical compositions but different aqueous phases were prepared. The aqueous phase of A was a solution of $M(NO_3)_2{\cdot}6H_2O$ (M = Mg, Zn or Ni, 0.4 M) and $Al(NO_3)_3{\cdot}9H_2O$ (0.125 M), while the aqueous phase of B was an NH_3 solution (5.0 M for the MgAl HTlc samples and 1.25 M for the NiAl and ZnAl HTlc samples).

Microemulsions A and B were prepared by dispersing CTABr (12.5 g, 0.034 mol) and *n*-butanol (15.5 mL, 0.169 mol) in isooctane (36.2 mL, 0.219 mol). A calculated volume of aqueous solution was added to each of these mixtures to obtain the desired water-to-surfactant molar ratio, R_w, and oil-to-water molar ratio, R_o. Both systems became clearly transparent.

The double-microemulsion processing route was then carried out by mixing equal volumes of the two initial microemulsions, A and B, to obtain the precipitation of MgAl, NiAl and ZnAl HTlcs in the reverse micelles. The resulting system (μAB) was stirred at room temperature for 15 min, after which it became cloudy and was aged at 25 °C or 75 °C for 8–15 h. After aging, the particles were recovered by centrifuging (12000 rpm for 10 min) and a semitransparent gel was obtained. The gel was washed with isooctane (1×30 mL), water (2×30 mL) and a methanol/chloroform mixture (1:1, v/v; 3×30 mL) and then dispersed in water or dried at 60 °C under oil pump vacuum to give a fine powder.

Characterization of Nanoparticles: The morphology of the MgAl HTlc nanoparticles present in the gel was investigated with a Jeol 2010 transmission electron microscope (TEM), operating at 200 kV. A small drop of the dispersion of the gel in water was deposited on a copper grid precoated with a Formvar film and then evaporated in air at room temperature.

The particle size distribution of the MgAl HTlc nanoparticles suspended in deionized water was determined with an Accusizer 770 (PSS Inc., Santa Barbara, CA, U.S.A.).

Atomic force microscopy (Solver-Pro, NT-MDT) measurements were carried out in semicontact conditions by using a 190–325 kHz cantilever having a 10 nm radius. The aqueous dispersions of the HTlc samples were sonicated for 30 min and then deposited on mica support by spin coating (4000 rpm, 20 s).

The powder morphology was obtained with a Philips XL30 scanning electron microscope (SEM). A drop of the dispersion of the gel in water, acetone or a methanol/chloroform mixture (1:1) was deposited on a holder, and the solvent was left to evaporate at room temperature. The samples were metallized with gold.

Dried powders were studied with chemical analysis, X-ray powder diffraction, thermal analysis and BET N_2 adsorption.

Metal analyses were performed by Varian 700-ES series inductively coupled plasma-optical emission spectrometers (ICP-OES) using solutions prepared by dissolving the samples in concentrated HNO_3 and then properly diluted. The carbon content was determined by elemental analysis using EA 1108 CHN FISONS instruments.

To determine the Br^- counterion content, a given amount of sample (≈ 100 mg) was equilibrated in a Na_2CO_3 solution (20 mL, 1 M) for 12 h. The solution was then analyzed for the Br^- content with a Dionex 2000 ion chromatograph equipped with an ionic conductivity detector.

The XRPD patterns were taken with a Philips X′PERT PRO MPD diffractometer operating at 40 kV and 40 mA, a step size of 0.0170 2Theta degree and a step scan of 20 s, using the Cu-K_α radiation and an X′Celerator detector.

Coupled thermogravimetric and differential thermal analyses were performed with a Netzsch STA 449C apparatus, in air flow and heating rate of 10 °C/min. The specific surface areas were calculated according to the BET method from N_2 adsorption isotherms taken at 77 K with a computer-controlled Micromeritics ASAP 2010 instrument.

Supporting Information (see also the footnote on the first page of this article): TG/DTA curves of samples 1, 2 and 4 (Table 1).

Acknowledgments

The authors express their gratitude to Prof. L. Latterini for providing atomic force microscopy (AFM) measurements. Thanks are due to the University of Perugia (PRIN 2006) for financial support.

[1] a) A.-H. Lu, E. L. Salabas, F. Schüth, *Angew. Chem. Int. Ed.* **2007**, *46*, 1222; b) S. Kinge, M. Crego-Calama, D. N. Reinhoudt, *ChemPhysChem* **2008**, *9*, 20.
[2] a) R. Allmann, *Acta Crystallogr., Sect. B* **1968**, *24*, 972; b) H. F. W. Taylor, *Miner. Magn.* **1969**, *37*, 338.
[3] a) F. Trifirò, A. Vaccari, F. Cavani, *Catal. Today* **1991**, *11*, 173; b) V. Rives, *Layered Double Hydroxides: Present and Future*, Nova Science Publishers, New York, **2001**; c) W. Jones, S. P. Newman, *New J. Chem.* **1998**, *22*, 105; d) A. I. Khan, D. O'Hare, *J. Mater. Chem.* **2002**, *12*, 1; e) F. Leroux, C. Taviot-Guého, *J. Mater. Chem.* **2005**, *15*, 3628; f) P. S. Braterman, Z. P. Xu, F. Yarberry, in *Handbook of Layered Materials* (Eds.: S. M. Auerbach, K. A. Carrado, P. K. Dutta), Marcel Dekker, New York, **2004**, p. 373.
[4] a) L. Latterini, M. Nocchetti, U. Costantino, G. G. Aloisi, F. Elisei, *Inorg. Chim. Acta* **2007**, *360*, 728.
[5] a) A. Vaccari, *Appl. Clay Sci.* **1999**, *14*, 161; b) M. Turco, G. Bagnasco, U. Costantino, F. Marmottini, T. Montanari, G. Ramis, G. Busca, *J. Catal.* **2004**, *228*, 43.
[6] a) U. Costantino, V. Ambrogi, L. Perioli, M. Nocchetti, *Microporous Mesoporous Mater.* **2008**, *107*, 149; b) *Clays and Health, Clays in Pharmacy, Cosmetics, Pelotherapy, and Environmental Protection* Special Issue of *Appl. Clay Sci.* (Eds.: M. I. Carretero, G. Lagaly), **2007**, p. 36.
[7] a) U. Costantino, F. Montanari, M. Nocchetti, F. Canepa, A. Frache, *J. Mater. Chem.* **2007**, *17*, 1079; b) F. R. Costa, M. Saphiannikova, U. Wagenknecht, G. Heinrich, *Adv. Polym. Sci.* **2008**, *210*, 101.
[8] a) J. H. Choy, S.-H. Hwang, J. M. Oh, *Solid State Ionics* **2002**, *151*, 285; b) Z. P. Xu, G. S. Stevenson, C. Q. Lu, G. Q. Lu, P. F. Bartlett, P. P. Gray, *J. Am. Chem. Soc.* **2006**, *128*, 36; c) X. Duan, D. G. Evans, *Chem. Commun.* **2006**, 485; d) V. Rives, P. Benito, F. M. Labajos, *Cryst. Growth Des.* **2006**, *6*, 1961; e) K. Okamoto, T. Sasaki, T. Fujita, N. Iyi, *J. Mater. Chem.* **2006**, *16*, 1608; f) Z. Liu, R. Ma, Y. Ebina, N. Iyi, K. Takada, T. Sasaki, *Langmuir* **2007**, *23*, 861; g) R. Ma, Z. Liu, K. Takada, N. Iyi, Y. Bando, T. Sasaki, *J. Am. Chem. Soc.* **2007**, *129*, 5257; h) P. Gunawan, R. Xu, *J. Mater. Chem.* **2008**, *18*, 2112.
[9] a) D. O'Hare, G. Hu, *J. Am. Chem. Soc.* **2005**, *127*, 17808; b) G. Hu, N. Wang, D. O'Hare, J. Davis, *Chem. Commun.* **2006**, 287; c) D. O'Hare, G. Hu, N. Wang, J. Davis, *J. Mater. Chem.* **2007**, *17*, 2257; d) S. Liu, D. Chen, K. Zhang, J. Li, N. Zhao, *Int. J. Hydrogen Energy* **2008**, *33*, 3736.

[10] a) F. Bellezza, A. Cipiciani, U. Costantino, F. Marmottini, M. A. Quotadamo, *Colloid Polym. Sci.* **2006**, *285*, 19; b) M. Husein, E. Rodil, J. Vera, *Langmuir* **2003**, *19*, 8467; c) C. Y. Tai, B. Y. Hsiao, H. Y. Chiu, *Colloids Surf. A: Physicochem. Eng. Aspects* **2004**, *237*, 105.
[11] M. A. Lopez-Quintela, *Curr. Opin. Colloid Interf. Sci.* **2003**, *8*, 137.
[12] C. Y. Tai, M. H. Lee, Y. C. Wu, *Chem. Eng. Sci.* **2001**, *56*, 2389.
[13] a) M. Zulauf, H. F. Eicke, *J. Phys. Chem.* **1979**, *83*, 480; b) P. Brochette, C. Petit, M. P. Pileni, *J. Phys. Chem.* **1988**, *92*, 3505; c) M. P. Pileni, *Langmuir* **2001**, *17*, 7476.
[14] U. Costantino, F. Marmottini, M. Nocchetti, R. Vivani, *Eur. J. Inorg. Chem.* **1998**, 1439.
[15] S. J. Gregg, K. S. W. Sing, in: *Adsorption, Surface Area and Porosity*, Academic Press Inc., London, **1982**.
[16] S. K. Yun, T. Pinnavaia, *J. Chem. Mater.* **1995**, *7*, 348.
[17] Q. Z. Yang, D. J. Sun, C. G. Zhang, X. J. Wang, W. A. Zhao, *Langmuir* **2003**, *19*, 5570.

Received: November 14, 2008
Published Online: April 30, 2009

